# Interactive Three-Dimensional Region of Interest Analysis of HMPAO SPECT Brain Studies

H. Richard Hooper, Alexander J. McEwan, Brian C. Lentle*, Tannis L. Kotchon, and Peter M. Hooper

*Department of Nuclear Medicine, Cross Cancer Institute, Edmonton, Alberta, Canada and Department of Statistics and Applied Probability, University of Alberta, Edmonton, Alberta, Canada*

An interactive computer program has been developed to align a three-dimensional region of interest (ROI) model to technetium-99m-hexamethylpropylenamine oxime ($^{99m}$Tc-HMPAO) single-photon emission computed tomography (SPECT) studies of the brain. The ROI model subdivides the human brain into fourteen discrete regions. A study was performed to determine normal ranges for HMPAO uptake in the ROIs defined by the model, and to assess the relative interobserver variability using the fitting program. HMPAO SPECT studies of twelve normal volunteers were independently analyzed by four observers. Small but significant differences between operators occurred primarily because of difficulty in defining the angle of the orbitomeatal plane on sagittal SPECT images. Despite this difficulty, the program and model have proven useful in defining ranges for normal cerebral perfusion in a healthy adult population. A study of a small group of patients with Alzheimer's dementia suggests that this procedure may be of use in the diagnosis of this disease.

**J Nucl Med 1990; 31:2046–2051**

The development of technetium-99m-hexamethylpropylenamine oxime ($^{99m}$Tc-HMPAO) single-photon emission computed tomography (SPECT) has offered the clinical community a safe, effective, and reproducible technique to measure human cerebral perfusion in vivo (*1,2*). Since the initial report of the scintigraphic appearance of a cerebrovascular accident by Ell and coworkers (*3*), many reports have described the qualitative appearance of the perfusion abnormalities in a wide range of disorders, including epilepsy (*4*), Alzheimer's dementia (*5*), Huntington's chorea (*6*), and congenital dysphasia (*7*).

Received Dec. 7, 1989; revision accepted May 17, 1990.

For reprints contact: Dr. H.R. Hooper, Department of Nuclear Medicine, Cross Cancer Institute, 11560 University Ave., Edmonton, Alberta, Canada, T6G 1Z2.

* Current address: Department of Radiology, Division of Nuclear Medicine, Vancouver General Hospital, Vancouver, British Columbia, Canada.

Most studies have only reported qualitative appearances of perfusion abnormalities. Where quantification has been attempted it has utilized multiple regions of interest (ROIs) drawn manually or generated by computer on multiple axial sections (*5,8–11*). These techniques are prone to partial volume errors and may lack reproducibility. Furthermore, the volumes defined may not correspond to functionally or anatomically distinct regions of the brain. Careful quantitative analysis of the tomographic data is necessary, however, to determine if subtle changes in regional count density are of clinical significance. Since rotating gamma camera SPECT systems map the full three-dimensional distribution of the radiotracer in the brain, three-dimensional, irregular ROIs should be used to analyze these studies. The manual drawing of such regions is, however, tedious, time-consuming, and can result in large systematic errors in image analysis, including inter-observer variability.

We have developed a three-dimensional ROI model that subdivides the human brain into fourteen discrete regions. This model can be interactively aligned to a SPECT brain study using a computer program developed in-house. This paper describes a pilot project in which this model and program were used to analyze the regional uptake of HMPAO in twelve normal volunteers. Using this model we have defined values for normal perfusion in a healthy adult population for use as a baseline against which pathophysiologic studies can be compared.

To assess the validity of the model in an abnormal patient population, we have compared the data obtained from our volunteer population with a small group of patients with Alzheimer's dementia.

## MATERIALS AND METHODS

### ROI Model and Analysis

The ROI model is illustrated in Figure 1. The model is made up of seven contiguous but nonoverlapping regions on each side of the brain. The seven regions are labeled as: superior and inferior frontal, parietal, occipital, temporal,

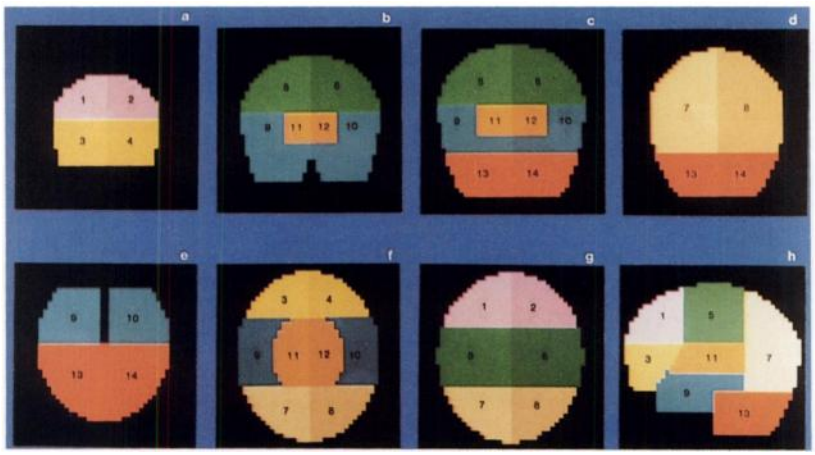

**FIGURE 1**
Sample slices through the ROI brain model. The region numbers are defined in Table 1. Coronal slices arranged from anterior to posterior (a) to (d). Transverse slices arranged from inferior to superior (e) to (g). Sagittal slice on right side (h).

midbrain, and cerebellar regions. Left and right regions are mirror images of each other. The regions are defined mathematically to correspond to general anatomical regions as illustrated in an atlas of cross sectional anatomy (*12*). The names associated with each region describe the general location of each ROI; while the regions were designed to represent cerebral anatomy as accurately as possible, the ROIs are not intended to correspond to exact anatomical structures. A Fortran 77 computer program that can be used to generate the ROI model is available (see Editor's note).

An analysis program has been developed to interactively fit the ROI model to a reconstructed HMPAO brain SPECT study as illustrated in Figure 2. Single coronal, transverse, or sagittal slices from the SPECT study are selected and displayed by the operator. The computer automatically overlays the SPECT slice with the appropriate ROI regions as defined by the model. Three different ROI overlay options are available to the operator: individual regions can be highlighted, the boundaries to all regions can be displayed, or only the outer ROI boundary may be displayed.

By entering either short-typed commands or single keystrokes, the operator can interactively change the shape and position of the ROI overlay, translating, compressing, expanding, or rotating the ROI model along or about any of the three orthogonal spatial coordinates. Using the external brain contour and various anatomical landmarks, the operator can quickly align the ROI overlay with the displayed SPECT slice. The geometric transformations are cumulative, however, and apply to the full three-dimensional model. Thus, when a new slice from the SPECT study is displayed, the appropriate ROI overlay is automatically calculated using the current geometric transformations. By displaying a few orthogonal frames from the SPECT study and aligning the ROI map on each frame, an operator can quickly align the ROI model with the patient study in all three dimensions. It should be noted that individual regions cannot be modified independently, nor can new regions be defined using the fitting program.

Once an operator is satisfied with the ROI fit to a particular SPECT study, the program calculates the total number of counts and volume (in voxels) in each region defined by the model; several composite regions (e.g., left and right frontal, total cerebellum) are also calculated. The results are displayed and printed. In order to minimize partial volume effects, voxels lying on ROI boundaries are subdivided amongst the nearest ROIs using a three-dimensional linear interpolative weighting.

The fitting program was developed on a Picker PCS computer running under the TSX operating system. The complete fitting and calculation procedure for one HMPAO SPECT study typically takes from 7 to 10 min.

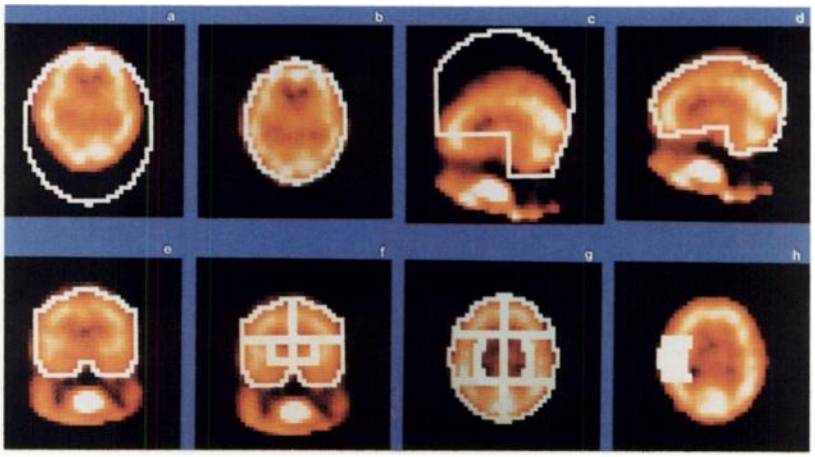

**FIGURE 2**
Example of the procedure used to fit the ROI model to a HMPAO brain SPECT study. The model is first overlaid on a transverse slice (a), then interactively fitted to the outer brain contour (b). A sagittal slice is then displayed (c) and the ROI overlay adjusted to fit this image (d). Other transverse, sagittal, or coronal slices can be displayed and used to fine tune the ROI fit. The final fit is displayed for a coronal slice (e,f), and a transverse slice (g,h). The outer ROI border is displayed in (a) through (e), the borders of all the ROI regions are displayed in (f) and (g), and only the ROI corresponding to the right temporal region is shown in (h).

### Volunteer Studies

SPECT studies were performed on twelve normal volunteers, three women and nine men, between 24 and 47 yr of age. The volunteer group was made up of physicians, nuclear medicine technologists, and university students. None had a history of psychiatric illness or of serious head injury. Appropriate written informed consent was obtained prior to each study.

Each volunteer was injected with ~550 MBq of $^{99m}$Tc-HMPAO. Projection images were obtained using a rotating gamma camera (General Electric, 400AC/T, Milwaukee, WI) equipped with a low-energy general-purpose parallel-hole collimator and interfaced to a commercial nuclear medicine computer system (Picker PCS-512, Solon, OH). Sixty-four images were obtained over 360° of rotation; each image was acquired for 40 sec and stored as a 64 × 64 matrix.

The projection images were prefiltered using a two-dimensional, image dependent Metz filter (*13–15*). The one-dimensional frequency domain form of this filter is defined as:

$$M(f) = [1 - (1 - H(f)^2)^X]/H(f), \qquad \text{Eq. 1}$$

where f is the spatial frequency, and H(f) a generalized exponential of the form:

$$H(f) = \exp(-f^P/S).$$

The function H(f) can be considered to be a parameterized representation of the system's modulation transfer function, and hence the parameters P and S are most sensitive to the collimator and isotope used. For these studies, the parameter values P = 1.4 and S = 30 were used. The parameter X controls the roll-off of the filter at higher frequencies, and was determined for each study using the criteria of King et al. (*15*).

Transverse images were reconstructed from the prefiltered projection images using filtered backprojection with a simple ramp filter, and the transverse images reformatted into coronal and sagittal planes for display and analysis. The reconstructed images were not corrected for attenuation.

The reconstructed SPECT studies for the twelve volunteers were independently analyzed by four operators trained to use the ROI fitting program described above. Counts from the 14 ROIs were standardized in two ways: by dividing by the total brain count (model 1) and by dividing by the total cerebellar count (model 2). The values obtained from the twelve volunteers were used to derive normal ranges of values for each region and operator (Fig. 3) using the two standardization protocols.

We have also attempted to demonstrate the errors associated with the technique, and to assess inter-observer variability. For each region, the standardized counts were modeled as the sum of an operator effect, a study effect, and an error term. Errors were assumed to be jointly normal and uncorrelated between the 48 operator-study cases. Examination of the residuals from the two fitted models revealed no departures from model assumptions, i.e., both models appear to be adequate for the purposes of this study.

The hypothesis of no operator effect and the hypothesis of no study effect were tested under both models. Univariate F-tests were performed separately for each region and four different multivariate tests, which take into account the joint variation in all regions, were also carried out. The tests check for operator and study effects within the context of additive models. The univariate tests do this separately for each region; the multivariate tests jointly using all regions. Anderson (*16*) presents a comparison of the power functions of the four multivariate tests.

### Studies of Patients with Alzheimer's Dementia

To assess the usefulness of the fitting program in an abnormal patient population, a small group of patients with Alzheimer's dementia was also studied. HMPAO SPECT studies were performed on seven patients with a history of progressive mental impairment. Four female and three male patients (mean age of 77.5 yr, range 69–85 yr) were included in this population. All patients had a history of progressive dementia and fulfilled the criteria for probable Alzheimer's disease (*17*). The images were assessed qualitatively according to previously published criteria (*5*). Quantitative and statistical analysis was performed using the same techniques as described in the volunteer section, except that only one operator analyzed the images.

## RESULTS

The region numbers used in the models are described in Table 1, with region numbers being defined sequen-

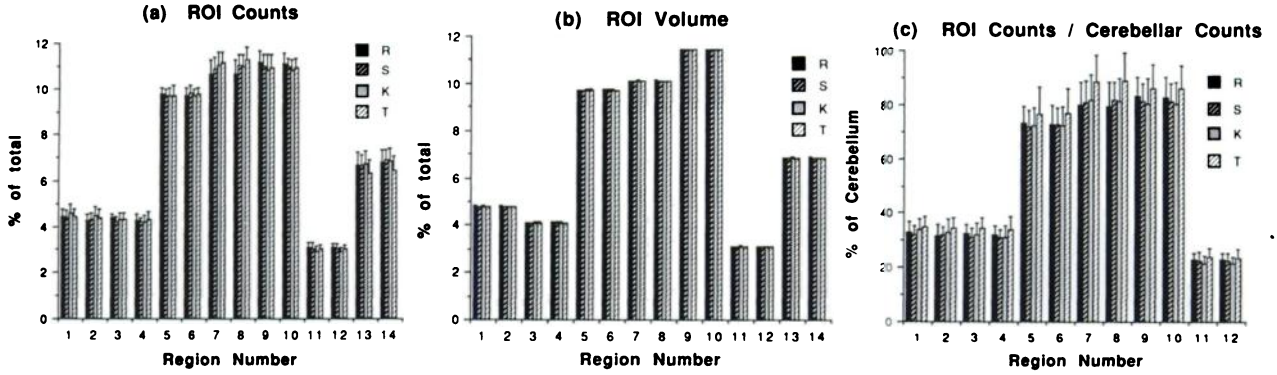


**FIGURE 3**
Means and standard deviations of the normalized ROI values over the twelve volunteers for each of the four operators (R,S,K,T). The error bars indicate 1 s.d. from the mean. (a) ROI counts as a percentage of total brain counts; (b) ROI volume as a percentage of total brain volume; and (c) ROI counts as a percentage of total counts in the cerebellum.

**TABLE 1**
Regions Defined by the ROI Brain Model

| Region number | Region name |
|---|---|
| 1 | Right superior frontal |
| 2 | Left superior frontal |
| 3 | Right inferior frontal |
| 4 | Left inferior frontal |
| 5 | Right parietal |
| 6 | Left parietal |
| 7 | Right occipital |
| 8 | Left occipital |
| 9 | Right temporal |
| 10 | Left temporal |
| 11 | Right midbrain |
| 12 | Left midbrain |
| 13 | Right cerebellum |
| 14 | Left cerebellum |

tially. The means and standard deviations in the measured ROI values over the twelve volunteers are summarized for each operator in Figure 3. ROI counts as a percentage of total counts are plotted in Figure 3A, ROI volume as a percentage of total volume in Figure 3B, and ROI counts as a percentage of total counts in the cerebellum in Figure 3C. The results of the statistical tests, in which an additive model was used to assess the interoperator and inter-study variability, are summarized in Table 2.

The quantitative results for the seven patients with Alzheimer's dementia are displayed and compared with volunteer data in Figure 4. Table 3 lists the p values for lower counts, relative to the total cerebellum, in total (i.e., right plus left) frontal, parietal, occipital, and temporal regions for these patients. All p values $< 0.1$ are listed, although only values $< 0.05$ should be considered significant.

Qualitatively the images of six of the seven patients showed some variation from previously published normal patterns of distribution of activity. Patients 1, 3, 4, and 7 showed evidence of cortical thinning, with the deficits being most evident in the temporal, parietal, and occipital regions. Patient 2 showed diffuse and equivocal frontal and parietal thinning, and Patient 6 showed generalized cortical thinning associated with one small focal defect in the left occipital lobe. The images for Patient 5 were considered normal.

**TABLE 2**
Statistical Analysis of Variability in Regional Uptake of HMPAO

| | p values | | | |
|---|---|---|---|---|
| | Model 1* | | Model 2† | |
| | Operator | Study | Operator | Study |
| Univariate F-tests: | | | | |
| Right superior frontal | 0.201 | 0.001 | 0.091 | 0.001 |
| Left superior frontal | 0.328 | 0.017 | 0.118 | 0.001 |
| Right inferior frontal | 0.415 | 0.246 | 0.079 | 0.002 |
| Left inferior frontal | 0.585 | 0.001 | 0.066 | 0.001 |
| Right parietal | 0.673 | 0.000 | 0.063 | 0.000 |
| Left parietal | 0.652 | 0.000 | 0.070 | 0.000 |
| Right occipital | 0.025 | 0.000 | 0.010 | 0.000 |
| Left occipital | 0.002 | 0.000 | 0.004 | 0.000 |
| Right temporal | 0.111 | 0.000 | 0.013 | 0.000 |
| Left temporal | 0.089 | 0.000 | 0.015 | 0.000 |
| Right midbrain | 0.147 | 0.000 | 0.059 | 0.000 |
| Left midbrain | 0.075 | 0.006 | 0.082 | 0.001 |
| Right cerebellum | 0.019 | 0.000 | — | — |
| Left cerebellum | 0.027 | 0.000 | — | — |
| Multivariate F Test: | | | | |
| Wilks' lambda | 0.003 | 0.000 | 0.001 | 0.000 |
| Pillai trace | 0.003 | 0.000 | 0.002 | 0.000 |
| Hotelling-Lawley trace | 0.004 | 0.000 | 0.002 | 0.000 |
| Roy's Maximum root | 0.063 | 0.000 | 0.050 | 0.000 |

* Regional counts expressed as a fraction of total brain counts.
† Regional counts expressed as a fraction of total cerebellar counts.

## DISCUSSION

The development of an algorithm to quantify HMPAO SPECT images should increase the sensitivity and specificity of the imaging technique, particularly in the diagnosis of subtle disease where qualitative defects are not apparent. There are now several reports in the literature where semi-quantitative analysis techniques have been utilized. While some of these have used computer-generated regions in multiple axial slices, most have required manual definition of multiple ROIs. These results are reported variously as left-to-right ratios, cortical-to-cerebellar ratios, or normal-to-abnormal ratios. The techniques used are often laborious and time-consuming, and may require several subjective

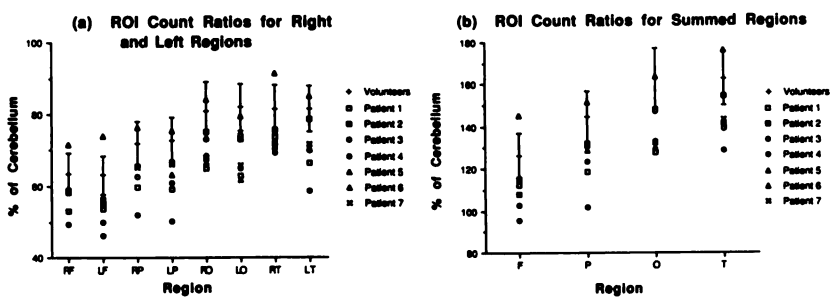


**FIGURE 4**
ROI counts as a percentage of total cerebellar counts in (a) separate left and right and (b) summed left plus right frontal, parietal, occipital and temporal regions, for the seven patients with Alzheimer's dementia and for the volunteers. The volunteer results illustrate the mean ±1 s.d. for the twelve volunteers. Both the patient and volunteer results are for one operator (operator S in Figure 3).

**TABLE 3**
Significance of Lower Relative Counts for Patients with Alzheimer's Dementia

| | p values from univariate F-tests | | | |
|---|---|---|---|---|
| Patient | Frontal | Parietal | Occipital | Temporal |
| 1 | — | 0.03 | 0.02 | 0.06 |
| 2 | 0.06 | — | — | — |
| 3 | 0.03 | 0.06 | — | 0.05 |
| 4 | 0.01 | 0.003 | 0.04 | 0.01 |
| 5 | — | — | — | — |
| 6 | — | — | 0.02 | 0.08 |
| 7 | — | — | 0.03 | 0.09 |

interactions on the part of the operator. There is considerable scope for the introduction of systematic errors from sampling difficulties, and perfusion in functionally or anatomically defined regions cannot truly be measured.

This pilot study was carried out to assess the performance of a three-dimensional ROI model and an interactive fitting program. Relative uptake values for $^{99m}$Tc-HMPAO have been calculated for the fourteen regions defined by the model. These numbers should be used cautiously. The sample size is small, and in order to precisely measure regional uptake it will be necessary to study a much larger group of volunteers, separated into subgroups by age and sex, and to control environmental factors such as visual and auditory stimuli following injection of the tracer. However, the data suggest that the values derived will be able to be used as part of a normal database against which a clinical population can be compared. Both calculated parameters (Fig. 3A and 3C) show uniform distribution of activity between the two cerebral and cerebellar hemispheres, and correspond with data obtained from PET studies of comparative regional cerebral perfusion (*18*). A study is presently underway to assess perfusion in a much larger population with a wide age range.

In this study, regional count data was normalized both to total brain activity and to total cerebellar activity. These normalization procedures should be appropriate for a broad range of neurologic disorders. Small, focal defects in one or two regions are most evident when total brain normalization is used. Large regional changes in perfusion, as expected for example in some psychiatric disorders, are most evident when total cerebellar normalization is used, since such disorders rarely effect cerebellar perfusion. Other normalization procedures could be implemented using the existing software, if required in a particular clinical situation.

Attenuation correction was not used in the present study because the correction algorithms used in our laboratory were not accurate enough for quantitative analysis. Most attenuation correction algorithms are quite sensitive to the location and shape of the body contour (*19,20*), and may introduce systematic errors into the reconstructed images. The main effect of not correcting for attenuation is to underestimate the activity in the midbrain region. If head size varied significantly, this could result in increased variability in relative counts in the midbrain regions. It was decided that this error was preferable to inadvertently misrepresenting the activity in the peripheral brain regions.

Various statistical tests were employed to assess interoperator variability in using the interactive fitting program. Analysis utilizing four multivariate F-tests revealed that, although the interoperator variability was less than the interstudy variability, the operator effect was still significant. Roy's Maximum Root test yielded substantially larger p-values for the operator effect than did the other three multivariate tests, which indicates that, while the operator effects appear to be jointly nonnegligible, there is no single linear combination of the operator effects that is substantial.

In reviewing the results from the various operators the primary cause of this inter-operator variability was revealed. All of the operators found the interactive fitting program easy to use, and in most cases could analyze a single volunteer study in between 10 and 15 min. The one operation which proved most difficult for the operators was defining the angle of the orbito-meatal plane on sagittal SPECT images. This parameter in turn defined the separation of the occipital and cerebellar regions. Thus, a large interoperator variability in defining this angle resulted in considerable variation in the relative counts in these regions. This effect is demonstrated in Table 2 in the univariate F-test results; the p-values for the operator effect under model 1 are lowest for the occipital and cerebellar regions. To overcome this problem, the fitting program will be modified so that operators can simply and accurately define the angle of the orbito-meatal plane.

The major question to be asked of any new analysis technique is whether it can discriminate between normal and pathophysiologic populations. Within the limited clinical data presented in this paper, we appear to have shown that variations from the normal pattern of perfusion can be quantified with our analysis technique.

The present patient data correlates with PET studies, where general reductions in both cerebral blood flow and glucose utilization have been reported, typically in the temporo-parietal regions, but sometimes in the fronto-parietal regions (*21*). These abnormalities have also been seen in studies utilizing xenon-133 (*22*).

In three patients whose SPECT images were qualitatively equivocal, the quantitative results produced using the fitting program were significantly lower than the normal ranges defined in the volunteer study. This suggests that the quantitative data may be diagnostic in patients with early Alzheimer's dementia. This thesis is currently being investigated in a larger, prospective study.

One patient demonstrated normal patterns of perfusion on both qualitative and quantitative analysis. This finding is in keeping with those of other authors who have found a range of normal values of cerebral perfusion in patients with Alzheimer's dementia (*5*). It should be remembered that the cause of dementia is difficult to confirm antemortem.

## CONCLUSIONS

An interactive computer program has been developed to align a three-dimensional ROI model to SPECT brain studies. A pilot study performed to assess the utility of this program revealed that it was simple to learn and use, and could provide useful quantitative information regarding the relative regional uptake of $^{99m}$Tc-HMPAO. Statistical analysis demonstrated that there was a significant difference in results obtained by different operators, although this variability was smaller than the range of results for different volunteers. The differences between operators occurred primarily because they had difficulty defining the angle of the orbitomeatal plane on sagittal SPECT images. The fitting program is currently being modified to overcome this difficulty.

To assess the validity of the fitting program in an abnormal patient population, quantitative results for a small group of patients with Alzheimer's dementia were compared with the volunteer data. Most of the patients had significantly lower uptake in the total frontal, parietal, occipital, and/or temporal regions, which suggests that this procedure may be of use in the diagnosis of Alzheimer's dementia.

***Editor's Note:*** A copy of the computer program utilized in this study can be obtained by sending a written request along with a self-addressed, stamped envelope to: Grant Banks, The Society of Nuclear Medicine, 136 Madison Ave., New York, NY 10016-6760.

## REFERENCES


1. Costa DC, Ell PJ, Cullum ID, Jarritt PH. The in vivo distribution of $^{99m}$Tc-HM-PAO in normal man. *Nucl Med Comm* 1986; 7:647–658.
2. Leonard J-P, Nowotnik DP, Neirinckx RD. Technetium-99m-d,l-HM-PAO: a new radiopharmaceutical for imaging regional brain perfusion using SPECT—a comparison with iodine-123 HIPDM. *J Nucl Med* 1986; 27:1819–1823.
3. Ell PJ, Jarritt PH, Cullum I, et al. A new regional cerebral blood flow mapping with $^{99m}$Tc-labeled compound. *Lancet* 1985; ii:50–51.
4. Biersack HJ, Stefan H, Reichmann K, et al. HM-PAO brain SPECT and epilepsy. *Nucl Med Comm* 1987; 8:513–518.
5. Perani D, Di Pietro V, Vallar G, et al. Technetium-99m-HM-PAO-SPECT study of regional cerebral perfusion in early Alzheimer's disease. *J Nucl Med* 1988; 29:1507–1514.
6. Reid IC, Besson JAO, Best PV, Sharp PF, Gemmel HG, Smith FW. Imaging of cerebral blood flow markers in Huntington's disease using single photon emission computed tomography. *J Neurol Neurosurg Psych* 1988; 51:1264–1268.
7. Denays R, Tondeur M, Foulon M, et al. Regional brain blood flow in congenital dysphasia: studies with technetium-99m-HM-PAO SPECT. *J. Nucl Med* 1989; 30:1825–1829.
8. Buell U, Stirner H, Braun H, Kreiten K, Ferbert A. SPECT with $^{99m}$Tc-HM-PAO and $^{99m}$Tc-pertechnetate to assess regional cerebral blood flow (rCBF) and blood volume (rCBV). Preliminary results in cerebrovascular disease and interictal epilepsy. *Nucl Med Comm* 1987; 8:519–524.
9. Podreka I, Suess E, Goldenberg G, et al. Initial experience with technetium-99m-HM-PAO brain SPECT. *J Nucl Med* 1987; 28:1657–1666.
10. Choksey MS, Costa DC, Iannotti F, Ell PJ, Crockard HA. $^{99m}$Tc-HM-PAO SPECT and cerebral blood flow: a study of $CO_2$ reactivity. *Nucl Med Comm* 1989; 10:609–618.
11. Nickel O, Nägele-Wöhrle B, Ulrich P, et al. RCBF-quantification with $^{99m}$Tc-HM-PAO-SPECT: theory and first results. *Eur J Nucl Med* 1989; 15:1–8.
12. Wagner M, Lawson TL. *Segmental anatomy—applications to clinical medicine.* New York: Macmillan; 1982.
13. King MA, Doherty PW, Schwinger RB, Jacobs DA, Kidder RE, Miller TR. Fast count-dependent digital filtering of nuclear medicine images. *J Nucl Med* 1983; 24:1039–1045.
14. King MA, Schwinger RB, Penney BC. Variation of the count-dependent Metz filter with imaging system modulation transfer function. *Med Phys* 1986; 13:139–149.
15. King MA, Glick SJ, Penney BC, Schwinger RB, Doherty PW. Interactive visual optimization of SPECT prereconstruction filtering. *J Nucl Med* 1987; 28:1192–1198.
16. Anderson TW. *An introduction to multivariate statistical analysis.* Second edition. New York: John Wiley & Sons; 1984:330–333.
17. McKhann, G, Drachman D, Folstein M, et al. Clinical diagnosis of Alzheimer's disease: report of the NINCDS-ADRDA Work Group under the auspices of Department of Health and Human Services task force on Alzheimer's disease. *Neurology* 1984; 34:939–944.
18. Phelps ME, Schelbert HR, Mazziotta JC. Positron computed tomography for studies of myocardial and cerebral function. *Ann Intern Med* 1983; 98:339–359.
19. Hosoba M, Wani H, Toyama H, Murata H, Tanaka E. Automated body contour detection in SPECT: effects on quantitative studies. *J Nucl Med* 1986; 27:1184–1191.
20. Macey DJ, DeNardo GL, DeNardo SJ. Comparison of three boundary detection methods for SPECT using Compton-scattered photons. *J Nucl Med* 1988; 29:203–207.
21. Duara R, Grady C, Haxby J, et al. Positron emission tomography in Alzheimer's disease. *Neurology* 1986; 36:879–887.
22. Metter EJ, Riege WH, Kameyama M, et al. Cerebral metabolic relationships for selected brain regions in Alzheimer's, Huntington's, and Parkinson's diseases. *J Cereb Blood Flow Metab* 1984; 4:500–506.